Bulletin of Plankton Society of Japan, 42 (1): 1-17, 1995

Physiological responses of Si-limited *Skeletonema costatum* to silicate supply with salinity decrease[1, 2]

TAMIJI YAMAMOTO[3] AND HARUHIKO TSUCHIYA[4]

Aichi Fisheries Research Institute, Gamagori, Aichi 443[3,4]

Abstract

Unsteady continuous culture of the diatom *Skeletonema costatum*, which is a dominant species forming red tides during the warm season in Mikawa Bay, was carried out. From the reported field observations, silicate concentration was considered to be the most plausible factor governing the biomass of *S. costatum* in the surface layer of the stratified water column. The two possible major processes involved in Si supply, i.e. from the bottom layer by wind mixing and by fresh water runoff, occurring in situ during this season were established by reciprocal replacement with a Si-sufficient media, with or without an accompanying salinity decrease of 5 ‰ to the Si-limited culture of *S. costatum*. The uptake rate of nitrate and phosphate per cell increased with Si limitation. Silicate limitation also caused several noticeable changes in the morphology of *S. costatum*. One of these morphological changes, cell elongation, made the cell quota of N and P larger than that of Si. On the other hand, silicate uptake rate per cell showed a sharp increase with increased Si supply and this elevated Si uptake rate was 5–9 fold that under Si-limited conditions. The degree of elevation of Si uptake was higher without an accompanying salinity decrease than with a salinity decrease, indicating that osmotic pressure may not be responsible for the uptake mechanism. Furthermore, Si-limited *S. costatum* showed higher growth rates when supplied Si with an accompanying salinity decrease than without a salinity decrease. Judging from these results, it is supposed that Si-depleted *S. costatum* grows faster in situ with Si supplied through river discharge, if the salinity is optimum for *S. costatum*, than through overturning of the water column due to wind mixing.

Key words: *Skeletonema costatum*, silicate, salinity, continuous culture, physiology

The marine diatom *Skeletonema costatum* is commonly found in coastal and estuarine areas, and constitutes a major fraction of the phytoplankton from late spring to summer (e.g. Braarud 1945, Hasle & Smayda 1960). In Mikawa Bay, Japan, red tides of this species occur almost all year round, and intensive occurrences of high cell densities are found during the warm season (Yamamoto et al. 1991). Maximum cell densities of red tides of this species reach to the order of 10^8 cells l^{-1}.

[1] Received: 29 September 1993/Accepted: 10 March 1995
[2] 塩分低下をともなう珪酸塩の供給に対する Si 制限 *Skeletonema costatum* の生理的応答
[3] 山本民次，現在: 広島大学生物生産学部
Present address: Faculty of Applied Biological Science, Hiroshima University, Higashi-Hiroshima 739
[4] 土屋晴彦，愛知県水産試験場

In Japan, the load of nitrogenous and phosphorous compounds from land to the coastal areas has increased through human activities, although in recent years the load of phosphorous compounds has decreased slightly because of concerted neighborhood action for the reduction of use of organic phosphorus-containing detergents as shown in Osaka Bay (Joh 1991). Therefore, in coastal and estuarine waters in Japan, silicate which is loaded at natural levels, may become a limiting factor for the growth of diatoms. Silicate concentration observed in Mikawa Bay (Tsuchiya & Yamamoto unpubl.) occasionally decreased to a limiting level (Thomas & Dodson 1975), as found in Narragansett Bay, U.S.A. (Pratt 1965) and Funka Bay, Japan (Tsunogai & Watanabe 1983).

In late spring, the water column of Mikawa Bay begins to stratify due to both an increase in the solar heat flux and an increase in freshwater runoff (Unoki 1984). The results of an eight-year monitoring program (1979–1986) revealed that red tides of *S. costatum* during the warm stratified season are induced by river water runoff or wind mixing or both (Tsuchiya & Yamamoto unpubl.). Salinity in the inner area of the bay usually fluctuated between 25 and 30 ‰, and the interval of fluctuation was around 2 to 3 days. A salinity decrease to 20 ‰ was often experienced, and values below 15 ‰ were occasionally observed. Variations in the cell density of *S. costatum* were inversely related to that of salinity, except when the salinity fell below 15 ‰. Moreover, silicate concentration increased with decreasing salinity, indicating that river water runoff is a major source of Si. Silicate concentration in the bottom layer was observed to be as high as 100 μg at l^{-1} during the stratified season (Tsuchiya & Yamamoto unpubl.). Therefore, mixing of the water column due to strong wind is assumed to be another mechanism for Si supply. According to Tsuchiya & Yamamoto (unpubl.), wind speeds greater than 5 m s^{-1} in daily average induce red tides of this species. Since wind is often accompanied by rainfall, the combination of river runoff and wind-induced mixing can be considered as the other case. In this case, however, estimation of the extent of relative contributions by river runoff and wind-induced mixing to the Si supply mechanism for phytoplankton growth is difficult. Therefore, two different cases, i.e. Si supply with and without salinity decrease were investigated in the present experiments.

These two different processes involved in Si supply may give rise to different physiological effects on diatom cells, because the exchange of dissolved materials through the cell membrane is considered to be related to the osmotic pressure of the cell. In the present study, we conducted continuous culture experiments using the diatom *S. costatum* which is a dominant species in Mikawa Bay. In the experiments, to replicate the two different processes of Si supply, Si-sufficient conditions with or without a corresponding salinity decrease were provided to Si-limited *S. costatum*. The purpose of the present study was to simulate the changes in silicate concentration with or without accompanying salinity decreases occurring in 2- or 3- day intervals in the estuarine environment of Mikawa Bay using an experimental system, and to observe how the salinity change affected both the nutrient uptake rate and the growth rate of *S. costatum*.

Materials and Methods

Strain and culture system

The diatom, *Skeletonema costatum*, which was isolated from Mikawa Bay, was used in the present experiment. The strain used was not clonal, because the use of a single clone might not be genetically representative of the natural population, as suggested by Gallagher (1980, 1982). The strain was kept in an axenic condition before the experiments both by repeated pipetting and transplantation of ca. 100–200 chains during the logarithmic growth phase. This preculture experiment was conducted using the HSHSi medium (Table 1) under 20° ±0.5° C, and continuous 100 and 150 μM m^{-2} s^{-1} light conditions (LI-1000 Quantum meter, Spherical Quantum Sensor : SPH, Li-cor Co. Ltd.) which are the same conditions as for the continuous culture experiment.

The continuous culture system used in the present study consisted of 4-liter Erlenmayer flasks, a peristaltic pump and a stirrer (Figure 1). All glassware, silicon tubes and teflon material were used either after heat sterilization (250° C, 2 h) or autoclaving (115° C, 30 min). The experiment was conducted twice (Expt I and II) using the same strain and the same system with the same medium except for the exclusion of silicate and phosphate (Table 1).

Culture media

Three kinds of culture media were prepared for each experiment using aged Mikawa Bay seawater (Table 1); high-salinity-low-Si medium (HSLSi), high-salinity-high-Si medium (HSHSi), and low-salinity-high-Si medium (LSHSi). These media simulate the usual conditions in the Si-depleted surface layer in the warm stratified season, Si enrichment by wind-induced mixing and Si enrichment by river

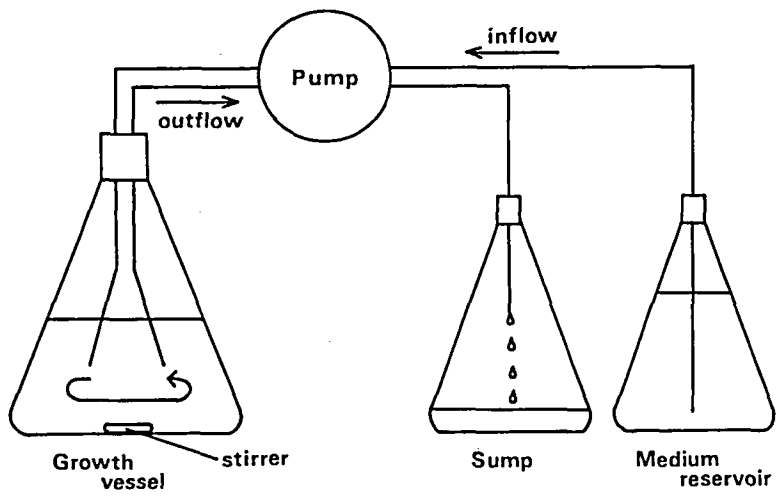

Fig. 1. Schematic diagram of the continuous culture system used in the present study.

Table 1. Composition of the three kinds of media used in the present experiments. HSLSi, high-salinity-low-Si medium; HSHSi, high-salinity-high-Si medium; and LSHSi, low-salinity-high-Si medium. Units are μg at l^{-1} for major nutrients, μg l^{-1} for vitamins. PII metal mixture is prepared according to Provasoli et al. (1957).

Medium	Salinity (‰)	Silicate-Si	Other components
Expt I			
HSLSi	30.2	13	NO_3-N, 150; PO_4-P, 10; B_1, 200; B_{12}, 0.5; H, 0.5; PII metal mixture, 2ml l^{-1}
HSHSi	30.2	300	as above
LSHSi	25.4	300	as above
Expt II			
HSLSi	23.6	16	NO_3-N, 150; PO_4-P, 12; B_1, 200; B_{12}, 0.5; H, 0.5; PII metal mixture, 2ml l^{-1}
HSHSi	23.6	300	as above
LSHSi	19.2	300	as above

runoff, respectively. The salinity of LSHSi was adjusted using distilled water. Since the phosphate (10 μg atP l^{-1}) added in Expt I seemed to be present at only very low levels during the Si-sufficient period and also slightly depleted concomitantly with Si in the first half of the Si-limited period, as shown later (Figure 2), the amount of added PO_4-P was increased by 2 μg atP l^{-1} in Expt II. The concentration of silicate-Si was 300 μg atSi l^{-1} in the high-Si media, whereas it was 13 μg atSi l^{-1} in the low-Si media of Expt I and 16 μg atSi l^{-1} in the low-Si media of Expt II. The pH of all the media were adjusted to 8.0 with a combination of diluted HCl and NaOH after the addition of nutrients.

These media were filtered twice, at the time of preparation and just before use, through a membrane filter (Toyo Advantech, pore size 0.2 μm) to minimize the bacterial contamination. Microscopic observation revealed that there was no contamination with bacteria and any other organisms in the system during the experiments.

Experiments

The first difference in the two series of experiments was salinity. In both experiments, a 5‰ salinity decrease was enforced, but it was from 30.2 to 25.4‰ in Expt I and from 23.6 to 19.2‰ in Expt II. A 5‰ salinity decrease most probably occurs in the estuarine region of Mikawa Bay as described above. The second difference in the two experiments was the sampling interval. In Expt I, sampling was done once a day at 09:00–10:00, while in Expt II it was done twice a day at 09:00–10:00 and 15:00–16:00. The purpose of shortening the sampling interval was to elucidate short-term physiological variations.

Precultured 1.9-liter *S. costatum* was transferred into the growth vessel, and the experiment was conducted with a dilution rate of 1.0 d^{-1} for 20 days in Expt I and for 18 days in Expt II. The experiments were conducted at 20±0.5°C and at a continuous illumination of ca. 100 μM m^{-2} s^{-1} in Expt I and ca. 150 μM m^{-2} s^{-1} in Expt II. White fluorescent lamps were used as the light source and the light intensity

was measured with a spherical quantum sensor (LI-1000 Quantum meter, Spherical Quantum Sensor : SPH, Li-cor Co. Ltd.). The 32-year average (1963–1994) of surface temperatures monitored in front of the Aichi Fisheries Research Institute, located on the northeastern coast of Mikawa Bay, was 20.1°C for the last ten days of May. The 17-year average (1974–1990) for atmospheric irradiance, recorded at Nagoya near the bay, was 946 μE m^{-2} s^{-1} for the last ten days of May (National Astronomical Observatory 1993). Supposing the reflection at the sea surface is 50% (Parsons et al. 1984), the irradiance under the surface becomes 473 μE m^{-2} s^{-1}. The extinction coefficient is calculated to be 0.525 m^{-1} from $K=2.1/T$ (K, extinction coefficient; T, transparency; Parsons et al. 1984) using the average transparency of 4 m in this season (Unoki 1984). Depths of ca. 3 m and ca. 2 m were calculated for 100 and 150 μE m^{-2} s^{-1}, respectively, supposing an exponential decrease in irradiance in the water column (Parsons et al. 1984). The temperature and irradiance values used in the present experiments were chosen to correspond to the above outlined conditions in the surface layer of Mikawa Bay in late May.

The input medium was replaced when it was determined that cell density had reached a maximum in the high-Si medium or a minimum in the low-Si medium. Therefore, parameters like cell density and nutrients were in an "unsteady" condition (cf. Burmaster 1979) during the transient phase. A vacuum pump was used during the 1-h sampling period to terminate nutrient uptake by the phytoplankton in the outflow medium. The amount of chlorophyll *a* (Chl *a*) was determined fluorometrically by the method of Yentsch & Menzel (1963). Nitrate, phosphate and silicate were analysed by the methods described by Strickland & Parsons (1972).

Calculation of nutrient uptake rate and growth rate

The change in nutrient concentration S in the growth vessel for time t (day) is described as follows,

$$dS/dt=D(S_{in}-S_{out})-\rho X. \quad (1)$$

The change of biomass in the growth vessel is expressed as

$$dX/dt=(\mu-D)X. \quad (2)$$

Where, the parameters are
S_{in}: input nutrient concentration (μg at l^{-1}),
S_{out}: output nutrient concentration (μg at l^{-1}),
X: biomass in the growth vessel (cells l^{-1}),
ρ: nutrient uptake rate by *S. costatum* (μg at $cell^{-1}$ d^{-1}),
μ : specific growth rate (d^{-1}),
D: dilution rate (d^{-1}).

In practice, the left-hand side of the equations (1) and (2) were approximated by $\Delta S_{out}/\Delta t$ and $\Delta X/\Delta t$, then ρ^i and μ^i between t^i and t^{i+1} were determined as

$$\rho^i=[D\{S_{in}^{i+1}-(S_{out}^{i}+S_{out}^{i+1})/2\}-(\Delta S_{out}/\Delta t)]/\{(X^i+X^{i+1})/2\}, \quad (1)'$$

and

$$\mu^i=(\Delta X/\Delta t)/X^i+D. \quad (2)'$$

When the steady state is maintained in the system, μ will approach D and $\rho = D(S_{in}-S_{out})/X$, then the cell quota ($Q$) can be calculated as

$$Q=(S_{in}-S_{out})/X, \tag{3}$$

and practically as

$$Q^i=\{S_{in}{}^i-(S_{out}{}^{i-1}+S_{out}{}^i)/2\}/\{(X^{i-1}+X^i)/2\}. \tag{3}'$$

During the experiments, the steady state was judged in practice by a less than 10 % variation in cell number during successive days. In Expt II, it was judged using the data from two successive mornings, because sampling on a twice-a-day-basis included their inherent diel variation. Steady state conditions were obtained on Day 4–5, 8–9, 15–16 and 19–20 in Expt I, and on Day 2–3, 7–8, 17–18 in Expt II. Microscope photographs were taken during the steady state conditions, and the average cell size was determined for 20 cells. However, the cell quota was calculated only for those cases where the concentration of nutrient concerned also varied less than 10 %, even if judgement of steady state condition was plausible on the basis of variations in cell density. Consequently, calculations of cell quota were made for Day 4–5, 15–16 and 19–20 for Si and N, and for Day 8–9 for Si, N and P in Expt I. They were made for Day 7–8 and 17–18 for N, and for Day 2–3 for Si, N and P in Expt II.

Results

Expt I

During the course of Expt I, peaks in cell density, $4.4\times10^8 l^{-1}$and $4.1\times10^8 l^{-1}$ were found on the 8th day in HSHSi and on the 20th day in LSHSi, respectively (Figure 2a). On the other hand, minimum cell densities were $1.2\times10^8\ l^{-1}$ on the 5th day and $0.94\times10^8\ l^{-1}$ on the 16th day, both in the HSLSi culture. Variations in Chl *a* concentration showed a similar pattern to the cell density, ranging from 70 μg l^{-1} on the 16th day to 160 μg l^{-1} on the 9th day (Figure 2a). However, Chl *a* content per cell tended to increase with Si-limitation, with a range of $2.6\text{–}8.1\times10^{-7}$ μg (Figure 2a).

Concentrations of silicate in the growth vessel varied in the range of 2.8–220 μg atSi l^{-1} (Figure 2b). Nitrate and phosphate concentrations varied in the ranges of 35–97 μg atN l^{-1} and 0.10-3.0 μg atP l^{-1}, respectively (Figure 2b). Nitrate and phosphate concentrations increased with Si-limitation, while they became low during the period of sufficient supply of Si. In both Si-sufficient periods, phosphate concentration became very low at a value of ca. 0.1 μg atP l^{-1}, which may indicate that phosphate is a limiting factor in those periods. These increasing and decreasing trends in nutrient concentration apparently follow the Liebig's low of minimum, i.e., the surplus portions of nitrate and phosphate at HSLSi are left-over due to depression of N- and P-uptake by Si-limitation.

The specific growth rate (μ) calculated from variations in cell numbers showed a rapid increase when the medium was changed from HSLSi to HSHSi or LSHSi; 1.9 d^{-1} for HSHSi and 2.3 d^{-1} for LSHSi (Figure 3a). After a rapid increase over the first day, the cell-division rate gradually slowed down and became equivalent to the dilution rate in 4 days for HSHSi and in 3 days for LSHSi. A small but detectable decrease in the growth rate was observed in the middle of the Si-limited

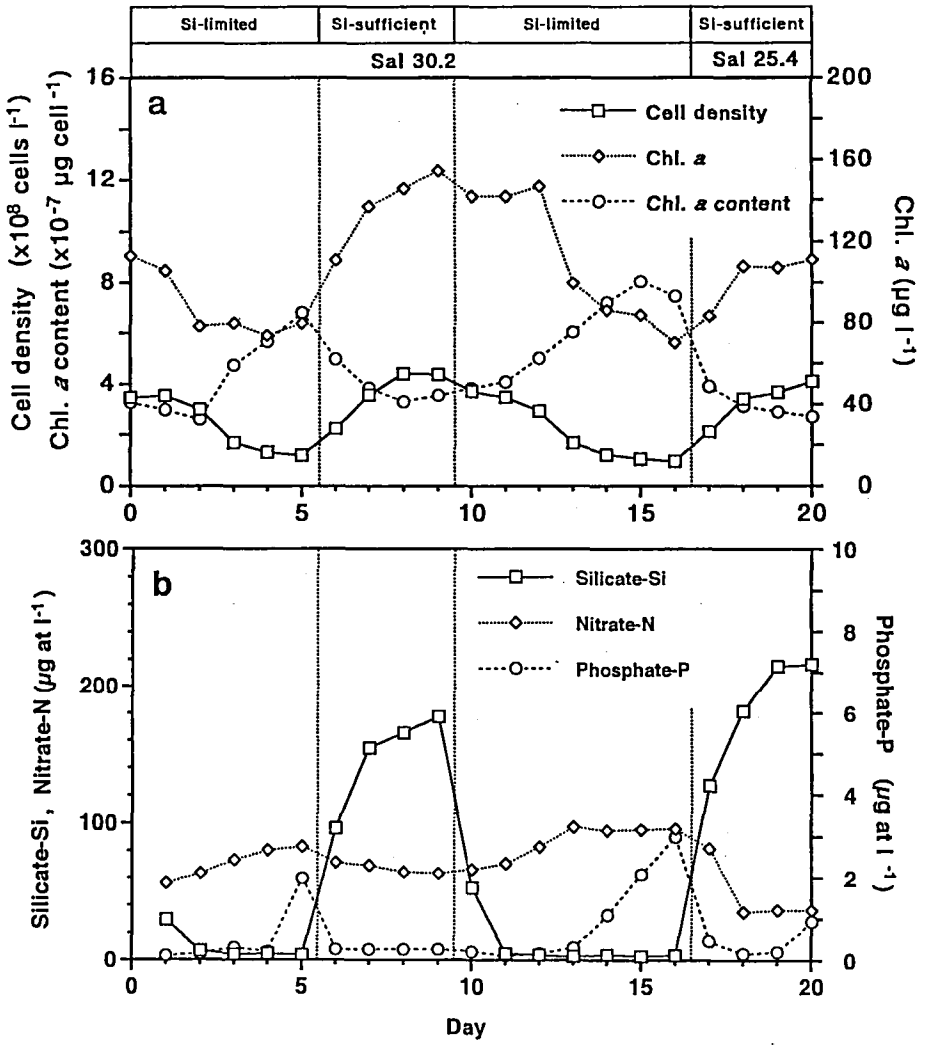

Fig. 2. Variations in (a) cell number, chlorophyll *a* and chlorophyll *a* content per cell of *S. costatum*, and (b) concentrations of silicate-Si, nitrate-N and phosphate-P during the course of continuous culture Expt I. Medium HSLSi for Days 1–5 and 10–16, medium HSHSi for Days 6–9, and medium LSHSi for Days 17–20. Refer Table 1 for the composition of the media.

period, i.e. the specific growth rate fell to 0.56 d^{-1} both on Day 2–3 and 12–13, which might indicate a mechanism regulating biomass to adapt to a Si-depleted environment.

Uptake rates of nitrate-N (ρ N) and phosphate-P (ρ P) increased with Si-limitation, still being high within a day after the addition of silicate, and gradually decreasing under Si-sufficient conditions (Figure 3b). Both ρ N and ρ P showed ca. 3-fold variations, ranging from 0.81×10^{-8} to 2.3×10^{-8} µg atN $cell^{-1}h^{-1}$ and from 0.89×10^{-9} to 2.8×10^{-9} µg atP $cell^{-1}\ h^{-1}$. The ρ N/Chl *a* and ρ P/Chl *a* also showed ca.

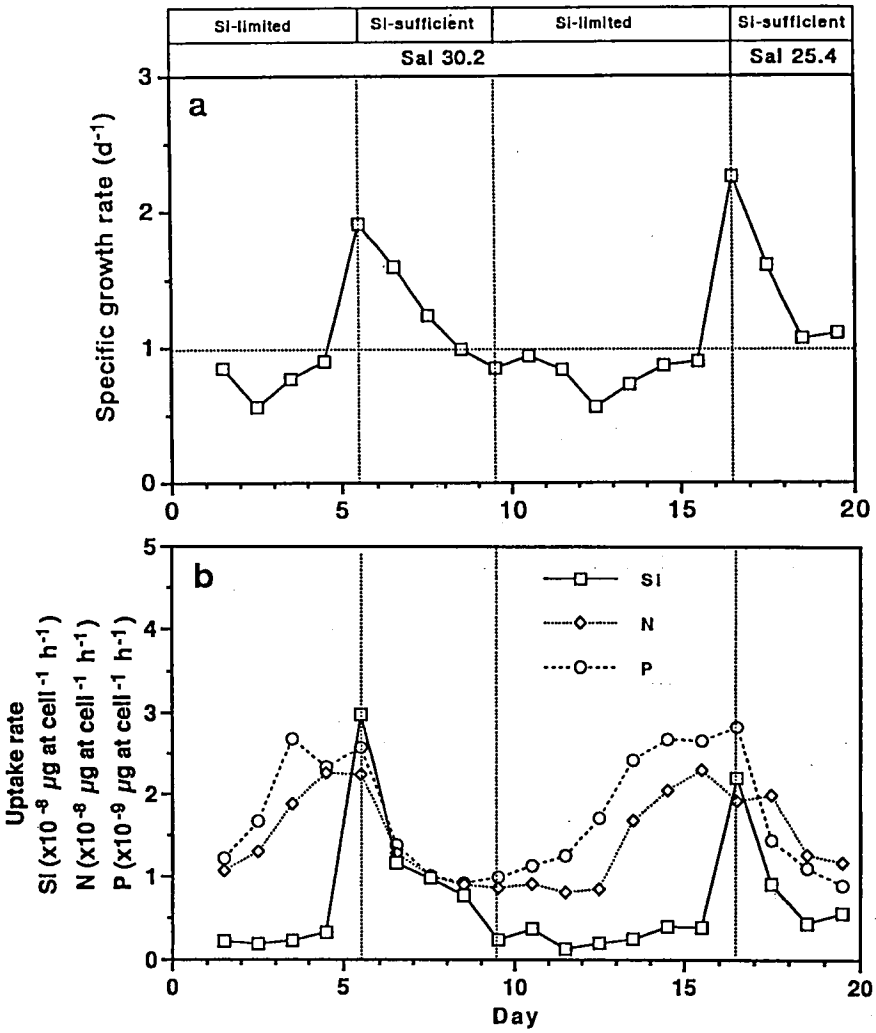

Fig. 3. Variation in (a) specific growth rate calculated from changes in cell density for a successive two days, and (b) the uptake rate of Si, N and P by *S. costatum*. Expt I. The dotted line at $\mu = 1$ in the upper figure denotes a sign where the specific growth rate is equivalent to the dilution rate.

3-fold variations with the ranges of 0.016–0.058 μg atN μgChl a^{-1} h^{-1} and 0.0027–0.0057 μg atP μgChl a^{-1} h^{-1}.

Unlike the curves for N and P uptake, ρ Si showed a sharp increase with increasing supply of silicate (Figure 3b); 3.0×10^{-8} μg atSi cell^{-1} h^{-1} at 30.2 ‰ and 2.2×10^{-8} μg atSi cell^{-1} h^{-1} at 25.4 ‰ and they were, respectively, ca. 9- and 6-fold greater than the values of the previous day. After the sharp increase, ρ Si gradually decreased to a constant level in the Si-sufficient media. Under the steady-state conditions in the HSLSi culture, the ρ Si obtained on Day 4–5 and 15–16 were at the same level, i.e. 0.33×10^{-8} and 0.39×10^{-8} μg atSi cell^{-1} h^{-1}, while they were slightly

different in the Si-sufficient steady states, i.e. 0.77×10^{-8} on Day 8–9 and 0.56×10^{-8} μg atSi cell^{-1} h^{-1} on Day 19–20, respectively. The ρSi/Chl *a* also showed greater variation than that of N or P at a magnitude of more than one order (0.0030–0.053 μg atSi μgChl a^{-1} h^{-1}).

The ρSi/ρN and ρSi/ρP ratios increased and decreased intermittently with changes in silicate concentration. The ρSi/ρN ratios were 0.35–1.3 under Si-sufficient conditions, while they were 0.12–0.41 under Si-limited conditions. The same trend was observed for ρSi/ρP ratios; 4.0–12 under Si-sufficient conditions, and 0.86–3.3 under Si-limited conditions. On the other hand, the ρN/ρP ratio was relatively constant compared to the ρSi/ρN and ρSi/ρP ratios, with a range of 5.0–14 and an average of 8.8, irrespective of the experimental conditions.

Expt II

In Expt II, cell density ranged from 0.92 to 6.0×10^{-8} cells l^{-1}(Figure 4a). The maximum cell density in Expt II was 1.3 times greater than that in Expt I, whereas the minimum cell density was similar to that in Expt I. The increase in the maximum cell yield might be attributable to the increased amount of added phosphate to the medium (Table 1). On the other hand, Chl *a* concentrations in Expt II were lower than those in Expt I, showing a range of 25–92 μg l^{-1}(Figure 4a). Light intensity in Expt II (ca. 150 μM m^{-2} s^{-1}) was higher than that in Expt I (ca. 100 μM m^{-2} s^{-1}). Adaptation of chloroplasts to the higher light intensity may cause the decrease in Chl *a* concentrations in Expt II, because even small numbers of photosystem units should be able to gather the light energy used for photosynthesis under higher light conditions. Chlorophyll *a* content per cell, $0.95–3.7\times10^{-7}$ μg, was also small compared to that observed in Expt I (Figure 2a). These differences can be caused not only by different cell numbers and Chl *a* concentrations but by cell size. Since the population used in Expt I had just undergone auxospore formation, cell size was apparently larger in Expt I (25 ± 2 μm in average diameter and 28 ± 6 μm in average length) than Expt II (5 ± 1 μm in average diameter and 9 ± 5 μm in average length).

Concentrations of silicate in the growth vessel varied in the range of 2.6–250 μg atSi l^{-1} (Figure 4b), which was roughly the same level as that in Expt I (Figure 2b). Nitrate concentration was also found to be at the same levels as those in Expt I, ranging from 75–120 μg atN l^{-1}. However, phosphate levels (0.47–6.2 μg atP l^{-1}) were high compared to those in Expt I because the amount added to the medium was increased by 2 μg at l^{-1}.

The maximum specific growth rate of 4.1 d^{-1} was obtained with the changing of the medium to LSHSi, and this value together with the value of another peak, 2.8 d^{-1} (Figure 5a), was greater than any in Expt I. These accelerated growth rates however were not sustained for even a day and returned to "normal" conditions in 18 h. This phenomenon appears to occur not by inherent diel variation but by an increase of cells in the phase before cell division, as will be discussed later. A slight decrease in the specific growth rate in the middle of the Si-limited period was again observed as in Expt I, and the values were 0.37 d^{-1} on Day 1 and 0.24 d^{-1} on Day 13.

The general trend in increases and decreases of ρN, ρP and ρSi was similar to that observed in Expt I. That is, ρN, ρP increased with Si-limitation, remained

high just after the addition of silicate, and gradually decreased under Si-sufficient conditions, while ρSi showed a sharp increase with the addition of silicate (Figure 5b). The ranges of ρN and ρP were 0.40–2.0$\times10^{-8}$ μg atN cell^{-1} h^{-1} and 0.46–3.4 $\times10^{-9}$ μg atP cell^{-1} h^{-1}, respectively. The uptake rate per Chl *a* unit was in the range of 0.035–0.060 μg atN Chl a^{-1} h^{-1} and 0.0031–0.012 μg atP Chl a^{-1} h^{-1}, respectively.

The increased ρSi values through Si supply were 4.2$\times10^{-8}$ μg atSi cell^{-1} h^{-1} at 23.6 ‰ and 3.6$\times10^{-8}$ μg atSi cell^{-1} h^{-1} at 19.2 ‰, and corresponded to a 5- and 6-fold

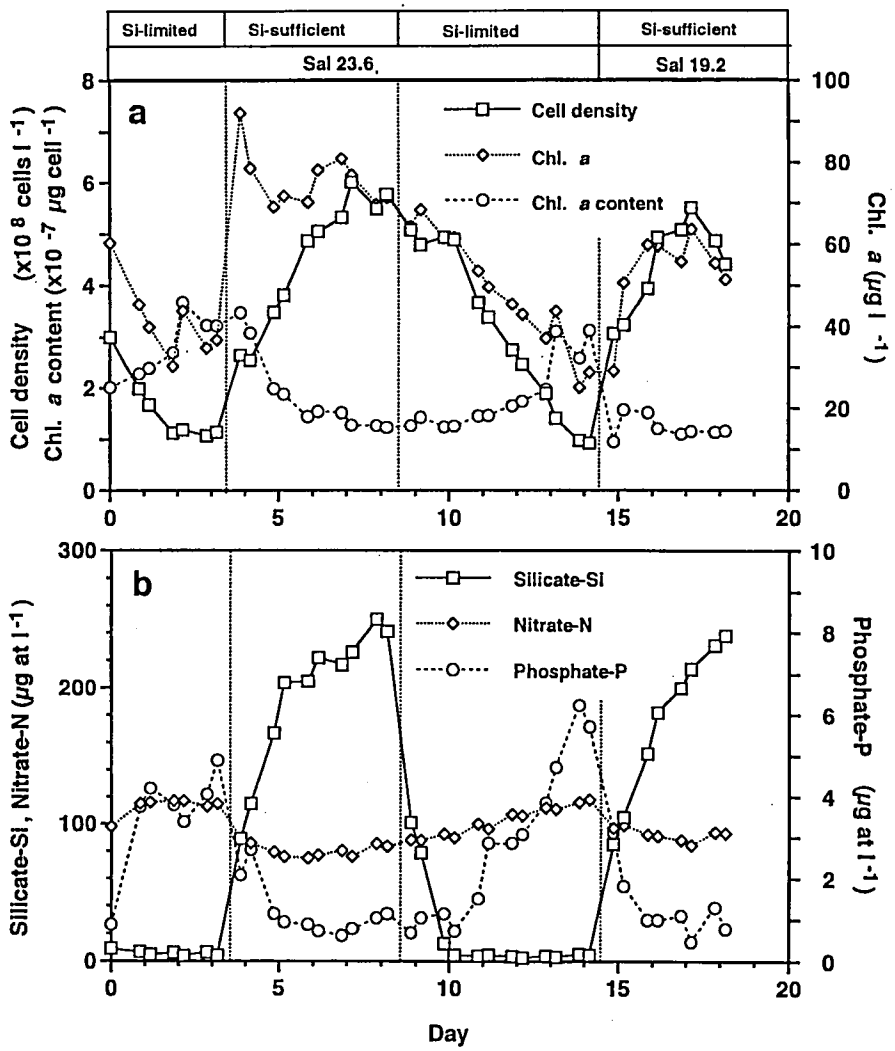

Fig. 4. Variations in (a) cell number, chlorophyll *a* and chlorophyll *a* content per cell of *S. costatum*, and (b) concentration of silicate-Si, nitrate-N and phosphate-P during the course of continuous culture Expt II. Medium HSLSi for Days 1–3 and 9–14, medium HSHSi for Days 4–8, and medium LSHSi for Days 15–18. Refer to Table 1 for the composition of the media.

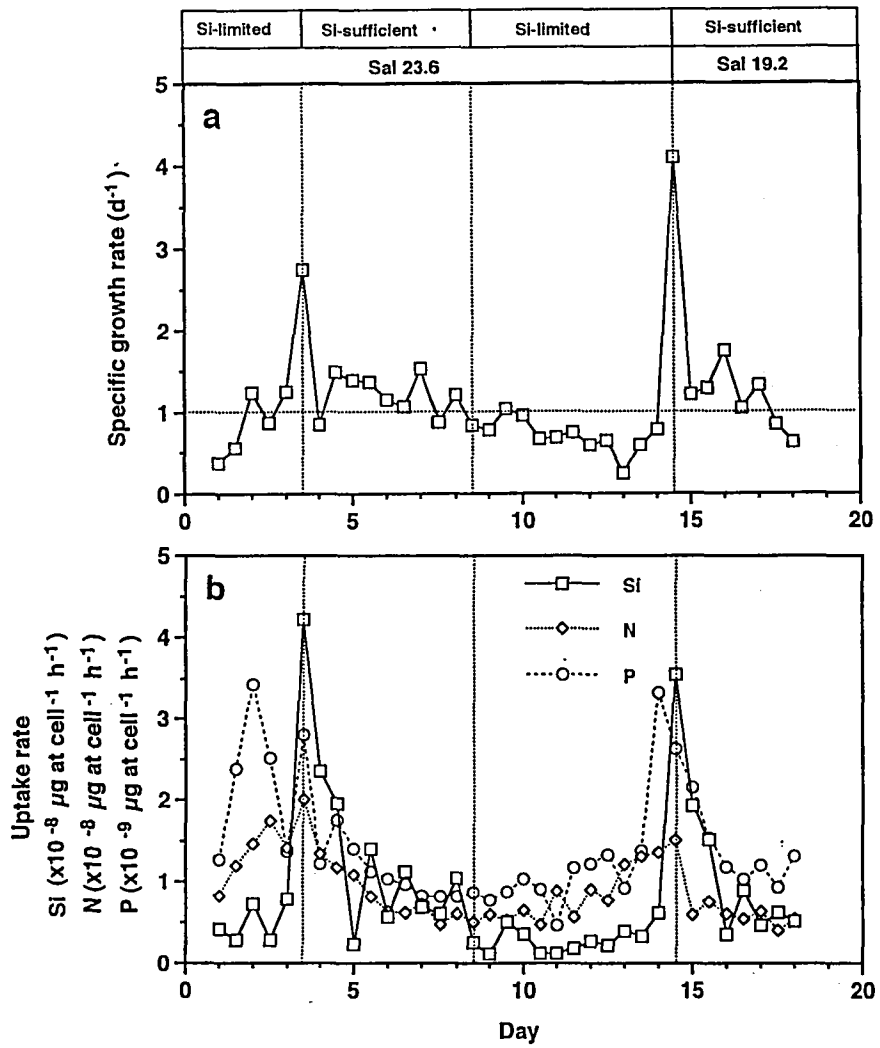

Fig. 5. Variations in (a) specific growth rate calculated from changes in cell density for a successive two samplings, and (b) the uptake rate of Si, N and P by *S. costatum*. Expt II. The dotted line at $\mu = 1$ in the upper figure denotes where the specific growth rate is equivalent to the dilution rate.

increase on previous values, respectively. However, the elevation of Si uptake rate terminated 1 or 2 days after the silicate was supplied (Figure 5b). From this result and the results of Expt I (Figure 3b), the bulk of the silicate needed for rapid cell division seems to be taken up within 1 or 2 days.

The general trends in the variation in the ratio of each of the two uptake rates was also similar to that observed in Expt I. The ρSi/ρN and ρSi/ρP ratios increased and decreased with the change in silicate concentration, whereas the ρN/ρP ratio was relatively constant at an average of 6.8 (range, 2.7–19). The ρSi/ρN ratio was 0.21–3.3 under Si-sufficient conditions, and 0.14–1.0 under the Si-limited

conditions. The maximum value, 3.3, was observed when HSLSi was applied. The ρSi/ρP ratios were 1.7–19 under the Si-sufficient conditions, while they were 1.1–5.7 under the Si-limited conditions.

Discussion

In both experiments, several morphological changes were observed under Si-limited conditions; the rod, the part of cell conjunction, was shortened or almost lost, the cell wall became thin, and the cell itself elongated. In Expt I, the average length of the cells was 31±5 μm in the Si-limited steady state compared to 25±3 μm in the Si-sufficient steady state. In Expt II, the average length of the cells was 12±3 μm in the Si-limited steady state, while it was 7±2 μm in the Si-sufficient steady state. However, there were no clear morphological differences between those from the two Si-sufficient media of different salinities. For *Cylindrotheca fusiformis*, increases in cell volume were observed both by Si-starvation (Lewin et al. 1966) and Si-limitation (Brzezinski et al. 1990). In the case of *Chaetoceros simplex* and *C. muellerii*, the percentage of daughter cells having no setae was increased by Si-limitation (Brzezinski et al. 1990). A spiky increase in phosphate concentration to P-limited *Monochrysis lutheri* led to an increase in their cell volume (Burmaster 1979), which is the reverse to the case of Si for *S. costatum* by Harrison et al. (1977) and the present study. According to the cell-cycle model by Brzezinski (1992), cell elongation can be interpreted through the increase in residence time in the phase before cell division. According to Brzezinski et al. (1990), a nutrient-limited cell moves slowly but continuously through the phases of the cell cycle, and the rate depends on the amount of limiting nutrient, whereas a nutrient-starved cell ceases the progression at the stage where the missing nutrient is required for completion of the cell-cycle. Several morphological changes, such as cell elongation, observed in the present study can be attributed to a slow progression through the cell-cycle.

The Q_{Si} obtained in the present experiments was significantly smaller (t-test, $p<0.05$, DF=3) in Si-limited steady state conditions (7.2–9.9×10^{-8} μg atSi cell^{-1} in both experiments) than in the Si-sufficient conditions (21 and 14×10^{-8} μg atSi cell^{-1} in Expt I) (Table 2). On the other hand, the Q_N was significantly greater (t-test, $p<0.05$, DF=5) in the Si-limited steady state (56×10^{-8} μg atN cell^{-1} in Expt I

Table 2. Silica, nitrogen and phosphorus cell quotas for *S. costatum* at steady state conditions for Si-limited (HSLSi) conditions and Si-sufficient conditions with two different salinities (HSHSi and LSHSi). ND: no data.

Condition (sal., ‰)	Q_{Si} ($\times10^{-8}$ μg at cell^{-1})	Q_N	Q_P	Q_{Si}/Q_N	Q_{Si}/Q_P	Q_N/Q_P
Expt I						
HSLSi (30.2)	7.2	56	ND	0.13	ND	ND
	9.9	56	ND	0.18	ND	ND
HSHSi (30.2)	21	21	2.2	1.0	9.7	9.7
LSHSi (25.4)	14	28	ND	0.50	ND	ND
Expt II						
HSLSi (23.6)	9.1	38	6.8	0.24	1.3	5.6
HSHSi (23.6)	ND	14	ND	ND	ND	ND
LSHSi (19.2)	ND	12	ND	ND	ND	ND

and 38×10^{-8} μg atN cell^{-1} in Expt II) than in the Si-sufficient steady state (21 and 28×10^{-8} μg atN cell^{-1} in Expt I and 14 and 12×10^{-8} μg atN cell^{-1} in Expt II). Therefore, the Q_{Si}/Q_N was found to be small in Si-limited steady state conditions (0.13 0.24) and large in Si-sufficient conditions (0.50–1.0) (Table 2). The Chl *a* content per cell was also higher in the Si-limited conditions compared to the Si-sufficient conditions (Figures 2a and 4a). The increase in intracellular materials can be attributed to cell elongation and the resulting increase in cell volume under Si-limited conditions. Similar results were reported by Harrison et al. (1977). However, the cell contents of Q_N and Chl *a* obtained during the Si-limited steady state in the present study were 2- to 3-fold greater than those reported by Harrison et al. (1977), while the values during the Si-sufficient steady state were at around the same level found in Harrison's study. This discrepancy may be attributable to the limited amount of silicate available.

In the present study, a 5–9 times increase in ρ Si was observed when silicate was supplied (Figures 3b and 5b). The maximum value of ρ Si obtained in Expt II (4.2×10^{-8} μg atSi cell^{-1} h^{-1}) exceeded by 3 times or more the maximum uptake rate ($1.0–1.3\times10^{-8}$ μg atSi cell^{-1} h^{-1}) reported by Harrison (1974) who also used a continuous culture method. On the other hand, Paasche (1973) reported 9.5×10^{-8} μg atSi cell^{-1} h^{-1} as the maximum silicate uptake rate of *S. costatum* by the conventional uptake experiment of inoculation of nutrient-starved cells into a series of media of various nutrient concentrations. The value reported by Paasche (1973) seems to be extraordinarily high compared to the results of Harrison (1974) and the present study. Paasche (1973) pointed out in his paper that there was little evidence for elevation in the uptake rate of Si as seen for N and P. This certainly does not correlate with the concept of a storage mechanism for Si as Paasche (1973) also mentioned. The absence of a storage mechanism for Si in diatoms was experimentally proven by Eppley et al. (1967), Busby & Lewin (1967) and Coombs & Volcani (1968). It is known that for pennate diatoms that silicate starvation leads to an increase in the percentage of cells at the phase before frustule formation in the cell cycle (Sullivan 1976, Okita & Volcani 1978, 1980, Blank & Sullivan 1979, Blank et al. 1986). According to recent information (Vaulot et al. 1987, Brzezinski et al. 1990), Si-limitation also leads to an increase in the percentage of cells at the phase before cell division in some centric diatom species. Brzezinski (1992) showed by the use of a computer model on *Thalassiosira weissflogii* that the maximum uptake rate of Si in cell-cycle dependent growth is about 8 times greater than that in continuous growth. Although there is no evidence that the the cell-cycle pattern of *S. costatum* is the same as that of *T. weissflogii*, the 5–9 times increase in ρ Si obtained in our experiments might be explained by an increase in the percentage of cells which need Si for cell division.

For *S. costatum* isolated from Woods Hole Harbor, the maximum photosynthetic rate was reached at a salinity of 15 ‰ in enriched seawater and at 20 ‰ in non-enriched seawater (Curl & McLeod 1961). The optimum salinity determined by the conventional batch culture method was 20 ‰ with no statistical difference between 10 and 20‰ (Takano 1963). Tsuruta et al. (1985) reported a much higher optimum value of ca. 27 ‰ for two isolates from the Yatsushiro Sea and Dokai Bay, Japan, where natural salinity ranges from 30.0 to 33.8 ‰ for the former and from 25.5 to 32.2 ‰ for the latter. From these results, they concluded that the two isolates were

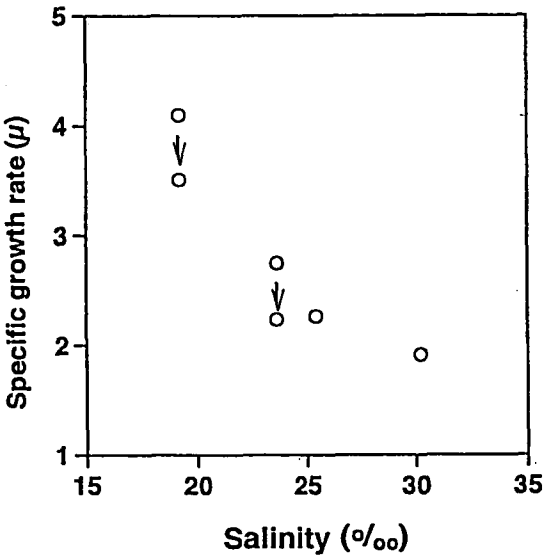

Fig. 6. Specific growth rates obtained at different salinity conditions. Data points at 25.4 ‰ and 19.2 ‰ were those obtained after decreasing salinity from 30.2 ‰ and 23.6 ‰, respectively. Arrows show the results of recalculation of the growth rate from an 18-h basis to a 24-h basis.

ecotypes adapted to the different environments. At any rate, growth of *S. costatum* is possible in a wide salinity range (Braarud 1951, Takano 1963), even in 5 ‰ provided a constant salinity is maintained (Brand 1984). On the other hand, in experiments incorporating long-term salinity changes using the recent continuous culture method, Rijstenbil & Sinke (1989) observed that photosynthetic rates and growth rates decreased below 16 ‰. Their results correspond well to observations in Mikawa Bay in which no growth of *S. costatum* was found below a salinity of 15 ‰ (Tsuchiya & Yamamoto unpubl.).

The exchange of dissolved materials through the cell membrane is closely related to the osmotic pressure of the cell. One of the focuses of the present experiments was to observe whether nutrient uptake rates would be accelerated or not by lowering the ambient salinity. In each experiment, the ρ Si value, elevated through Si supply was higher without a corresponding salinity decrease than with a salinity decrease, although the difference could not be tested statistically because of the lack of data. Rijstenbil & Sinke (1989) have discussed that nitrogen taken up is lost to a much larger degree under unsuitable salinity conditions. According to them, the optimum salinity for growth of *S. costatum* with respect to ammonium uptake was 18 ‰. With respect to silicate, *S. costatum* may also take up ambient silicate more efficiently at an optimum salinity of probably around 18 ‰. At any rate, the results of the two experiments indicate that osmotic pressure alone is not enough to allow effective silicate uptake in *S. costatum* cells.

The marked increases in μ following silicate addition were greater at low salinities; 4.1 d^{-1} at 19.2 ‰, 2.8 d^{-1} at 23.6 ‰, 2.3 d^{-1} at 25.4 ‰ and 1.9 d^{-1} at 30.2 ‰ (Figures 3a and 5a). Since the former two values were calculated on an 18-h basis, recalculation on a 24-h basis for comparison to the latter two values was carried out and the results were 3.5 d^{-1} and 2.2 d^{-1}, which however did not change the trend (Figure 6). Under conditions higher than the optimum salinity (probably ca. 18 ‰), rate processes should decrease with an increase in salinity. The highest

elevation in growth rate observed at the lowest salinity (19.2 ‰) seems to correspond to this. Judging from the change in specific growth rate to a salinity decrease with corresponding Si supply (Figure 6), it is supposed that Si-depleted *S. costatum* grows faster in situ with Si supplied through river discharge, if the salinity is optimum for *S. costatum*, than through overturning of the water column due to wind mixing.

Acknowledgments

We thank Dr. Y. Nakamura of the National Institute for Environmental Studies for his critical review of the manuscript and constructive comments. Thanks are also due to Prof. N. Rajendran for his critical review of the manuscript. This study was supported by the Fund for Research and Prediction of Red Tides in the Tokai Coastal Area of the Fisheries Agency.

Literature Cited

Blank, G. S., D. H. Robinson & C. W. Sullivan, 1986. Diatom mineralization of silicic acid. VII. Metabolic requirements and the timing of protein synthesis. *J. Phycol.*, **22**: 382–389.

Blank, G.S. & C.W. Sullivan, 1979. Diatom mineralization of silicic acid. III. $Si(OH)_4$ binding and light dependent transport in *Nitzschia angularis*. *Arch. Mikrobiol.*, **123**: 157–164.

Braarud, T., 1945. A phytoplankton survey of the polluted waters of inner Oslo Fjord. *Hvalrad. Skr.*, **28**: 1–142.

Braarud, T., 1951. Salinity as an ecological factor in marine phytoplankton. *Physiol. Plant.*, **4**: 28–34.

Brand, L. E., 1984. The salinity tolerance of forty-six marine phytoplankton isolates. *Est. Coast. Shelf Sci.*, **18**: 543–556.

Brzezinski, M. A., R. J. Olson & S. W. Chisholm, 1990. Silicon availability and cell-cycle progression in marine diatoms. *Mar. Ecol. Prog. Ser.*, **67**: 83–96.

Brzezinski, M. A., 1992. Cell-cycle effects on the kinetics of silicic acid uptake and resource competition among diatoms. *J. Plankton Res.*, **14**: 1511–1539.

Burmaster, D. E., 1979. The unsteady continuous culture of phosphate-limited *Monochrysis lutheri* Droop: Experimental and theoretical analysis. *J. exp. mar. Biol. Ecol.*, **39**: 167–186.

Busby, W. F. & J. C. Lewin, 1967. Silicate uptake and silica shell formation by synchronously dividing cells of the diatom *Navicula pelliculosa* (Bréb.) Hilse. *J. Phycol.*, **3**: 127–131.

Coombs, J. & B. E. Volcani, 1968. Studies on the biochemistry and fine structure of silica shell formation in diatoms. Chemical changes in the wall of *Navicula pelliculosa* during its formation. *Planta*, **82**: 280–292.

Curl, H. Jr. & G. C. McLeod, 1961. The physiological ecology of a marine diatom, *Skeletonema costatum* (Grev.) Cleve. *J. mar. Res.*, **19**, 70–88.

Eppley, R. W., R. W. Holmes & E. Paasche, 1967. Periodicity in cell division and physiological behavior of *Ditylum brightwellii*, a marine planktonic diatom, during growth in light-dark cycles. *Arch. Mikrobiol.*, **56**: 305–323.

Gallagher, J. C., 1980. Population genetics of *Skeletonema costatum* (Bacillariophyceae) in Narragansett Bay. *J. Phycol.*, **16**: 464–474.

Gallagher, J. C., 1982. Physiological variation and electrophoretic banding patterns of genetically different seasonal populations of *Skeletonema costatum* (Bacillariophyceae). *J. Phycol.*, **18**: 148–162.

Harrison, P. J., 1974. Continuous culture of the marine diatom *Skeletonema costatum* (Grev.) Cleve under silicate limitation. Ph. D. dissertation, 140 pp., Univ. Washington, Seattle.

Harrison, P. J., H. L. Conway, R. W. Holmes & C. O. Davis, 1977. Marine diatoms grown in chemostats under silicate or ammonium limitation. III. Cellular chemical composition and morphology of *Chaetoceros debilis, Skeletonema costatum*, and *Thalassiosira gravida*. *Mar. Biol.*, **43**: 19–31.

Hasle, G. R. & T. J. Smayda, 1960. The annual phytoplankton cycle at Drobak, Oslofjord. *Nytt. Mag. Bot.*, **8**: 53–75.

Joh, H., 1991. Change of marine environment of Osaka Bay due to coastal development. *Bull. coast. Oceanogr.*, **29**, 3–12. (In Japanese with English abstract)

Lewin, J. C., B. E. Reiman, W. F. Busby & B. E. Volcani, 1966. Silica shell formation in synchronously dividing diatoms. pp. 169-188. In *Cell Synchrony. Studies in Biosynthetic Regulation* (eds. Cammerson, I. L.& G. M. Pedilla). Academic Press, New York.

Okita, T. W. & B. E. Volcani, 1978. Role of silicon in diatom metabolism. IX. Differential synthesis of DNA polymerases and DNA-binding proteins during silicate starvation and recovery in *Cylindrotheca fusiformis*. *Biochim. Biophys. Acta*, **519**: 76–86.

Okita, T. W. & B. E. Volcani, 1980. Role of silicon in diatom metabolism. X. Polypeptide labelling patterns during the cell cycle, silicate starvation and recovery in *Cylindrotheca fusiformis*. *Expl. Cell. Res.*, **125**: 471–481.

Paasche, E., 1973. Silicon and the ecology of marine plankton diatoms. II. Silicate-uptake kinetics in five diatom species. *Mar. Biol.*, **19**: 262–269.

Parsons, T. R., T. Takahashi & B. Hargrave, 1984. Biological Oceanographic Processes. 330pp. Pergamon Press, Oxford, New York, Toronto, Sydney, Paris and Frankfurt.

Pratt, D. M., 1965. The winter-spring diatom flowering in Narragansett Bay. *Limnol. Oceanogr.*, **10**, 173–184.

Provasoli, L., J. J. A. McLaughlin & M. R. Droop, 1957. The development of artificial media for marine algae. *Arch. Mikrobiol.*, **25**: 392–428.

Rijstenbil, J. W. & J. J. Sinke, 1989. The influence of salinity fluctuation on the ammonium metabolism of the marine diatom *Skeletonema costatum* grown in continuous culture under continuous illumination. pp. 79–103. In *Growth and Nitrogen Metabolism of Marine Diatoms in Brackish Water in Response to Salinity Fluctuation*, Comm. Delta Inst. Hydrobiol. Res., 419 (ed. Rijstenbil, J. W.). OMI Grafisch Bedrijf, Utrecht.

Strickland, J. D. H. & T. R. Parsons, 1972. A Practical Handbook of Sea Water Analysis. *Bull. Fish. Res. Bd. Canada*, **167**, 310 pp.

Sullivan, C. W., 1976. Diatom mineralization of silicic acid. I. $Si(OH)_4$ transport characteristics in *Navicula pelliculosa*. *J. Phycol.*, **12**: 390–396.

Takano, H., 1963. Diatom culture in artificial sea water-1. Experiments on five pelagic species. *Bull. Tokai reg. Fish. Res. Lab.*, **37**: 17–25.

Thomas, W. H. & A. N. Dodson, 1975. On silicic acid limitation of diatoms in near surface waters of the eastern tropical Pacific Ocean. *Deep-Sea Res.*, **22**: 671–677.

Tsunogai, S. & Y. Watanabe, 1983. Role of dissolved silicate in the occurrence of a

phytoplankton bloom. *J. oceanogr. Soc. Japan*, **39**: 231–239.

Tsuruta, A., M. Ohgai, S. Ueno & M. Yamada, 1985. The effect of the chlorinity on the growth of planktonic diatom *Skeletonema costatum* (Greville) Cleve in vitro. *Bull. Jap. Soc. sci. Fish.*, **51**: 1883–1886. (In Japanese with English abstract)

Unoki, S., 1984. Naiwan no Butsuri-Kankyo. pp. 63–162. In *Naiwan no Kankyo Kagaku, Mikawawan, Isewan wo Chuushin toshite*, (ed. Saijo, Y.). Baifu Kan, Tokyo. (In Japanese)

Vaulot, D., R. J. Olson, S. Merkel & S. W. Chisholm, 1987. Cell-cycle response to nutrient starvation in two phytoplankton species, *Thalassiosira weissflogii and Hymenomonas carterae*. *Mar. Biol.*, **95**: 625–630.

Yamamoto, T., M. Ishida & H. Tsuchiya, 1991. Heisei 2 nen Ise-wan Mikawa-wan no Akashio Hassei Jōkyō. Aichi Suishi Kenkyu Gyoseki C, **84**: 50 pp. (In Japanese)

Yentsch, C. S. & D. W. Menzel, 1963. A method for the determination of phytoplankton chlorophyll and pheophytin by fluorescence. *Deep-Sea Res.*, **10**: 221–231.